Physicochemical Characterization of Aerosols in the Coastal Zone: Evidence of Persistent Carbon Soot in the Marine Atmospheric Boundary Layer (MABL) Background

Philippe Parent, Carine Laffon, Victor Trillaud, Olivier Grauby, Daniel Ferry, Alix Limoges, Tathy Missamou, Jacques Piazzola

atmosphere

MDPI

Article

Physicochemical Characterization of Aerosols in the Coastal Zone: Evidence of Persistent Carbon Soot in the Marine Atmospheric Boundary Layer (MABL) Background

Philippe Parent [1], Carine Laffon [1], Victor Trillaud [1], Olivier Grauby [1], Daniel Ferry [1], Alix Limoges [2], Tathy Missamou [2] and Jacques Piazzola [2,*]

[1] CNRS, Aix-Marseille Université, UMR 7325, CINAM, 13288 Marseille, France
[2] Mediterranean Institute of Oceanography [MIO UM 110], University of Toulon, CEDEX 09, 83041 Toulon, France
* Correspondence: piazzola@univ-tln.fr; Tel.: +33-494142082

Abstract: Aerosol particles in coastal areas result from a complex mixing between sea-spray aerosols locally generated at the sea surface by breaking waves and a continental component issued from natural and/or anthropogenic sources. The aim of this paper is to study how the aerosols mix in the coastal marine atmosphere to evaluate the impact of the background pollution on the atmospheric aerosols. To this end, we have carried out a qualitative analysis of particulate matter sampled at two French coastal areas using a non-destructive methodology combining scanning electron microscopy (SEM)/X-ray fluorescence, transmission electron microscopy (TEM), X-ray diffraction, and Raman spectroscopy. Our analysis shows a dominant contribution of anthropogenic aerosols through strong levels of submicronic carbon soot and sulfate particles, even observed when the aerosol is sampled during pure maritime-air mass episodes. Our results also evidence the non-mixing between sea-spray, mainly composed of coarse aerosol particles, and this anthropogenic particulate matter of smaller sizes.

Keywords: aerosols; sea-spray; carbon soot; sulfate aerosol

Citation: Parent, P.; Laffon, C.; Trillaud, V.; Grauby, O.; Ferry, D.; Limoges, A.; Missamou, T.; Piazzola, J. Physicochemical Characterization of Aerosols in the Coastal Zone: Evidence of Persistent Carbon Soot in the Marine Atmospheric Boundary Layer (MABL) Background. *Atmosphere* **2023**, *14*, 291. https://doi.org/10.3390/atmos14020291

Academic Editors: Haochi Che, Lu Zhang, Caroline Dang and Zengliang Zang

Received: 1 December 2022
Revised: 25 January 2023
Accepted: 28 January 2023
Published: 1 February 2023

1. Introduction

Atmospheric aerosol particles from natural or anthropogenic sources play a major role in many physicochemical processes in the lower troposphere important to the global climate [1]. They contribute to air and water pollution with adverse consequences for human health [2–4]. Air-quality monitoring agencies responsible for alerting the population are faced with difficulties related to the spatial and temporal variations and the variety of composition of these particles. In coastal areas, the aerosol concentrations result from a complex mixing of particles produced by natural processes of both continental and marine origin and anthropogenic particles emitted from urban and industrial activities. In particular, the Mediterranean coast constitutes a "Hot Spot" for studies on anthropogenic impact and future climate-change projections [5]. In such areas, the contribution of aerosols of marine origin must be considered specifically because they can interact physically and chemically with other types of aerosols and gases present in the air [6] and has a significant influence on the coastal urban air quality [7]. The few previous analyses on both aerosol concentration and composition in the coastal Mediterranean area available in the literature, indicate a rather homogeneous marine background concentration, whereas the anthropogenic contribution can vary significantly in the Western and the Eastern Mediterranean [8–11]. At the local scale, the estimation of aerosol sources and their atmospheric fate is a key for air quality prediction, but remains a significant scientific challenge [12,13]. The size of sea-spray particles can vary over a wide range, with a dimension at formation from sub-micrometric size to about 500 µm [14]. These particles consist of a mixture of

inorganic salts—primarily of sodium chloride (NaCl) and small amounts of other salts such as sulfate, calcium, and potassium—and organic compounds. The ability of particles to take up water, termed hygroscopicity, is determined by the particle's size and chemical composition. In terms of diameter change, the hygroscopic growth of inorganic sea salt is 8–15% lower than NaCl, most likely due to the difference in chemical composition [15], generally attributed to the internally mixed organic substances [16]. A dominant inorganic sea-spray contribution to sub-micron aerosol particle mass takes place during winter, while during periods of high biological activity the inorganic sea-spray is progressively replaced by organic matter and non-sea-salt (nss)-sulfate. However, due to a limited understanding of the mechanisms that control the transfer of organic matter from seawater to sea-spray, it is currently impossible to predict the organic composition of sea-spray in the Marine Atmospheric Boundary Layer (MABL) of coastal areas [17].

Thus, the main question raised first is: what is this aerosol made of? To obtain a better knowledge of the physical and chemical composition of the marine aerosols in these areas, and in particular the propensity to mix with organic compounds and anthropogenic aerosols of continental/urban origin, we have carried out a qualitative assessment of the properties of size-selected aerosols collected on two coastal sites located in the Atlantic and Mediterranean regions. We used scanning electron microscopy (SEM) coupled with energy dispersive X-ray (EDX) fluorescence analysis, transmission electron microscopy (TEM), X-ray diffraction, and Raman spectroscopy. Our results reveal the importance of the anthropogenic influence. We detected a strong and constant contribution of soot issued from maritime and urban/maritime traffic constituted of submicronic aerosols, along with high amounts of sulfate salt particles. These fine anthropogenic aerosols are clearly separated from the sea-spray aerosol. Consequently, we must consider large atmospheric lifetimes for these submicronic anthropogenic particles and, hence, strong health and climate risks for the near future. This improved knowledge of the aerosol mixing processes in the MABL of Mediterranean and oceanic coastal area will also allow a better modeling of the aerosol optical depth (AOD), an important input parameter of the climate models.

2. Material and Methods

2.1. Field Sites

Our experiments were carried out in two different geographical sites: the first one was located on the island of Porquerolles in the Toulon-Hyères bay on the French Mediterranean coast (Figure 1), between 6.15- and 6.25-degrees east longitude and at 43 degrees north latitude in the North-Western Mediterranean. The French Mediterranean coast represents a densely populated zone where large amounts of aerosol particles of anthropogenic origin are expected. A fine analysis of the meteorological conditions of the study area, as well the seasonal variations in aerosol concentrations were described in detail in Piazzola and Despiau [18]. The island of Porquerolles is exposed to air masses from the open sea, as well as to air masses originating over the European mainland, with a very short fetch, that represent continentally polluted conditions. If a strong contribution of sea-spray aerosols was noted even for offshore winds at short fetches [18], pollutants are much higher, even for long fetches, than in the Atlantic atmosphere. Previous work conducted by Piazzola et al. [5] showed the concomitant presence of sea-sprays and high levels of anthropogenic species such as nitrate. In Figure 2, the wind vectors recorded during the sampling period are reported. The SEM-REV site for multi-technology offshore testing is the second experimental site used in the present study (Figure 1). It is in Le Croisic in the Atlantic coastal zone, twenty kilometers from Nantes (47.294 N, 2.513 W). The two sites present very different characteristics in terms of meteorology and air mass influence. The station located on the island of Porquerolles is quite close to a very anthropized region, while the second one is under a large Atlantic influence most of the time.

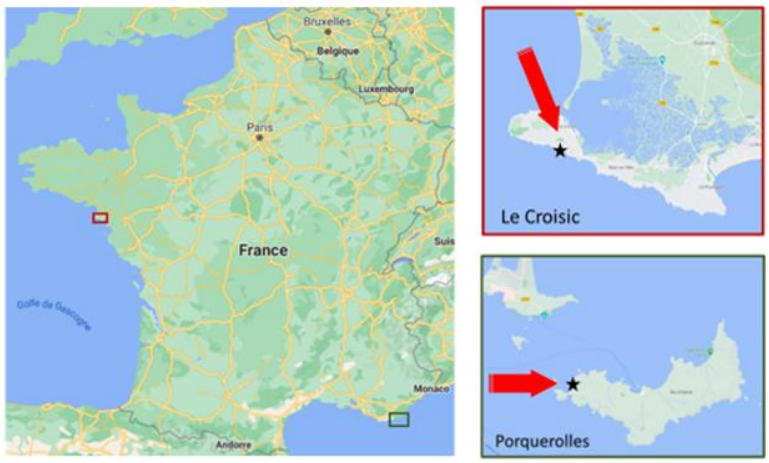

Figure 1. Geographical position of the two sampling sites (the stars).

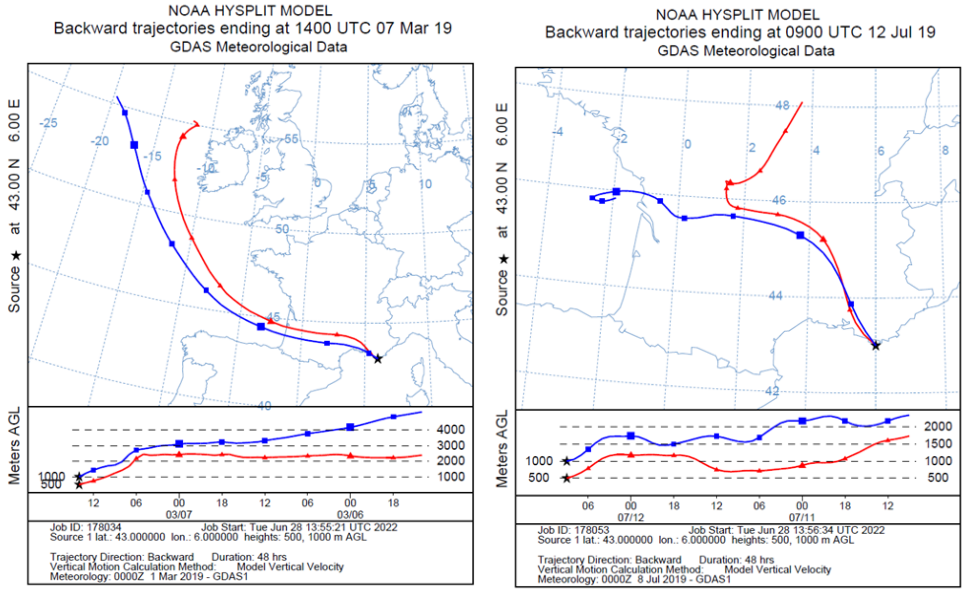

Figure 2. Air mass backtrajectories recorded during aerosol samplings made on the island of Porquerolles in March 2019 (P1, **left**)) and July 2019 (P2, **right**).

2.2. Analytical Sampling and Procedures

Aerosols were sampled in the atmosphere with a 13-stage low pressure cascade impactor (DLPI, DEKATI). This is a multi-jet device which operates at a nominal flow rate of 18.34 L/min with cut-off diameters (D50%) of 0.03 µm (called stage E1), 0.06 µm (E2), 0.11 µm (E3), 0.17 µm (E4), 0.26 µm (E5), 0.40 µm (E6), 0.65 µm (E7), 1.0 µm (E8), 1.6 µm (E9), 2.5 µm (E10), 4.4 µm (E11), 6.8 µm (E12), and 9.97 µm (E13) (DLPI impactor data-sheet, Dekati, Kangasala, Finland). At each stage, the aerosol accumulates on the substrate as impaction points, which are small deposits (<1 mm in diameter) located beneath the holes of the stage's metal sieve. To adapt the nature of the substrates to the physicochemical analysis, we simultaneously used polycarbonate membranes (Isopore 0.2 µm, Millipore, Burlington, MA, USA) and aluminum foils (CF-300 Dekati, Kangasala, Finland). The substrates were cut in half and arranged side by side on the collection stage. The aluminum substrates were used for Raman spectroscopy since polycarbonate induces an intense Raman signal which mixes with the spectrum of the collected particles. Several sets of samples were collected by the impactor between March 2019 and November 2020 in periods characterized by different meteorological conditions (Table 1). For each meteorological period presented in Table 1, we

have studied the properties of the corresponding air masses using numerical calculations of the air mass backtrajectories issued from the NOAA HYSPLIT model [19]. Figure 2 reports the air mass backtrajectories in the Mediterranean for the samplings conducted on the island of Porquerolles (P1 and P2 in Table 1), while Figure 3 shows the air mass backtrajectories recorded during the Atlantic experiments in Le Croisic (C4 to C7 in Table 1).

Table 1. List of samples collected using the impactor between March 2019 and January 2021 in the two experimental sites.

	Date	Site	Sampling Time	Wind Direction/Speed (ms^{-1})	Air Mass Origin	RH (%)	T (°C)
P1	07/03/2019	Porquerolles	24 H	W/2-7	OceanicContinental	60–92	10–15
P2	12/07/2019	Porquerolles	8H30	WNW/4-8.5	Continental	40–81	22–30
C4	09/07/2020	Le Croisic	15 H	W/5-8.5	Oceanic	67–95	23–16
C5	05/11/2020	Le Croisic	16 H	ENE/4-8	Continental	71–90	10–15
C6	17/11/2020	Le Croisic	17 H	SSE/2-4	Coastal	57–90	6–12
C7	18/11/2020	Le Croisic	18 H	NNW/2-7	Coastal	44–85	6–12

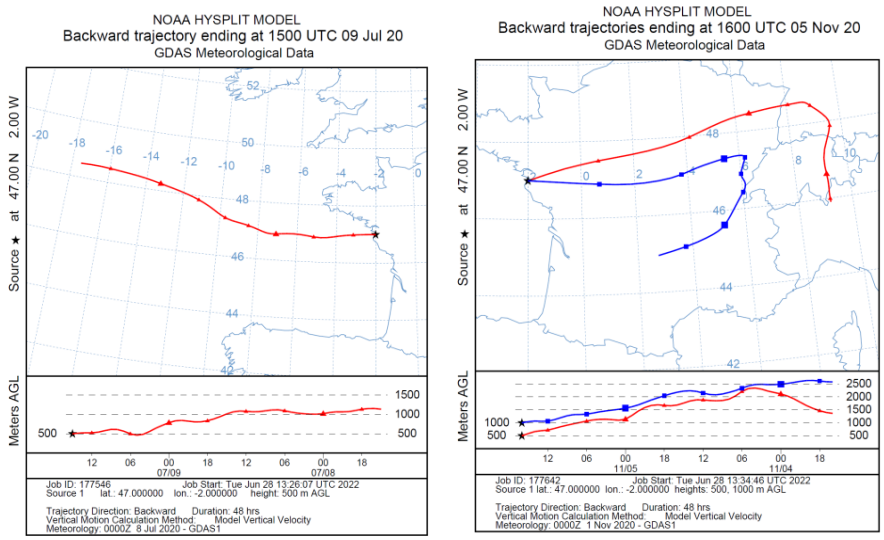

Figure 3. Air mass backtrajectories recorded during aerosol samplings made at Le Croisic in July (C4, **left**) and November 2020 (C5, **right**).

Episode P1 corresponds to a local wind direction varying from 220 to 270 degrees and dealing with somewhat recurrent conditions in the study area. The fetch for these wind directions can range from 100 km to unlimited fetch (open water conditions) and hence, deals with a strong marine influence. Sea breeze and land breeze can add to the synoptic air mass path. Episode P2 locally corresponds to a short 25 km-fetch on the island of Porquerolles (Figure 2). These conditions are typical of the study area and defined as "Mistral" conditions. They are associated with a high wind speed of northwestern origin. For episode P2, local winds often shift from North-west to South-west at night. This wind is dry and cold most of the time.

Scanning electron microscopy (SEM) was performed with a Jeol 7900F microscope. The images are acquired at low voltage between 1 and 5 keV. The elemental chemical analysis is obtained by analysis of the X-ray fluorescence (Energy Dispersive X-ray, EDX) measured with a Quantax FlatQuad detector. On a smaller scale, the aerosols were also characterized by transmission electron microscopy (TEM). For this, the filter is cut out around an impaction point; the particles are then dissolved in ethanol and dispersed by

ultrasound; a drop of the solution is placed on a microscope grid and left to evaporate. The TEM is a JEOL JEM-2010 at 200 kV (0.23 nm resolution), equipped with a LaB6 filament and a GATAN UltraScan 1000XP model 994 CCD camera. The GATAN Suite v.2.31 software was used for image analysis. X-ray diffraction (XRD) measurements were performed in transmission mode using a high-brightness rotating anode, Rigaku RU-200BH, (operating power 50 kV-50 mA) equipped with a double Osmic reflection mirror, and an image plate detector Mar345. The radiation used is Cu Kα at 1.5418Å, and the size of the beam is 0.5×0.5 mm^2. The Raman analysis are carried out with a Renishaw Reflex Invia micro-spectrometer equipped with a Leica DM2500M microscope. The characterizations were carried out at 785 nm with ×100 magnification, an 1800-line grating and a CCD detector.

3. Results

Whether in Porquerolles or in Le Croisic, we found a great similarity in the physico-chemical nature of the samples collected on the different days. The nature of the aerosol appears quite independent of the meteorological conditions (except, as we will see, on the aerosol load through atmospheric mixing). There was also no significant difference between the two sites of Porqueroles and Le Croisic, i.e., between a quasi-urbanized area (for the former) and a site exposed to Atlantic air masses (for the latter). Therefore, it is unnecessary here to make an extensive presentation of all those similar samples (104 in total), and it is more relevant to present in greater detail a selection of the samples collected at both sites that we found representative of our observations. Moreover, the nature of the sampled particles varied slowly between the successive impactor's stage; thus, we have simplified the size distribution into three broader ranges of size: fine modes (corresponding to stages E1–E5, 0.03–0.26 μm), intermediate modes (E6–E9, 0.40–1.6 μm), and coarse modes (E10–E13, 2.5–9.97 μm). In the following, we mainly present samples of these three ranges of size collected during two chosen days on the two sites, namely P1 (Porquerolles) and C4 (Le Croisic).

3.1. Coarse Modes

Figure 4 shows a characteristic SEM image of coarse modes collected on stages E10–E13 (D50% = 2.5–9.97 μm) on polycarbonate substrates; this is stage E13 (9.97 μm) of the P1 sample of Porquerolles (March 2019). Figure 4a,b present low and high magnification SEM images, respectively. Figure 4b presents the XRD spectrum of stage E13 of P1, whose main lines match with those of NaCl (rock salt, halite; red vertical lines). At low magnification, we observe an anisotropic distribution of small cubic or rectangular crystals, organized in a circle (circled in red on the image). Superimposed to the SEM image, the EDX mapping of sodium (Figure 4c) and chlorine (not shown) of these deposits confirms that they are NaCl crystals. They are left after liquid drops of sea-salt aerosol have dried under the airflow, delimiting the circular imprint [20]. No other particles such as soot or sulfate aerosol are detected by SEM and EDX inside or in the vicinity of these crystals, indicating the absence of internal mixing of the sea-salt aerosol particles with other particulate matter. For comparison, Figure 4d,e show SEM images of stages E13 of the P2 sample of Porquerolles (July 2019) and the C4 sample of Le Croisic (July 2020), where similar NaCl crystallites were observed.

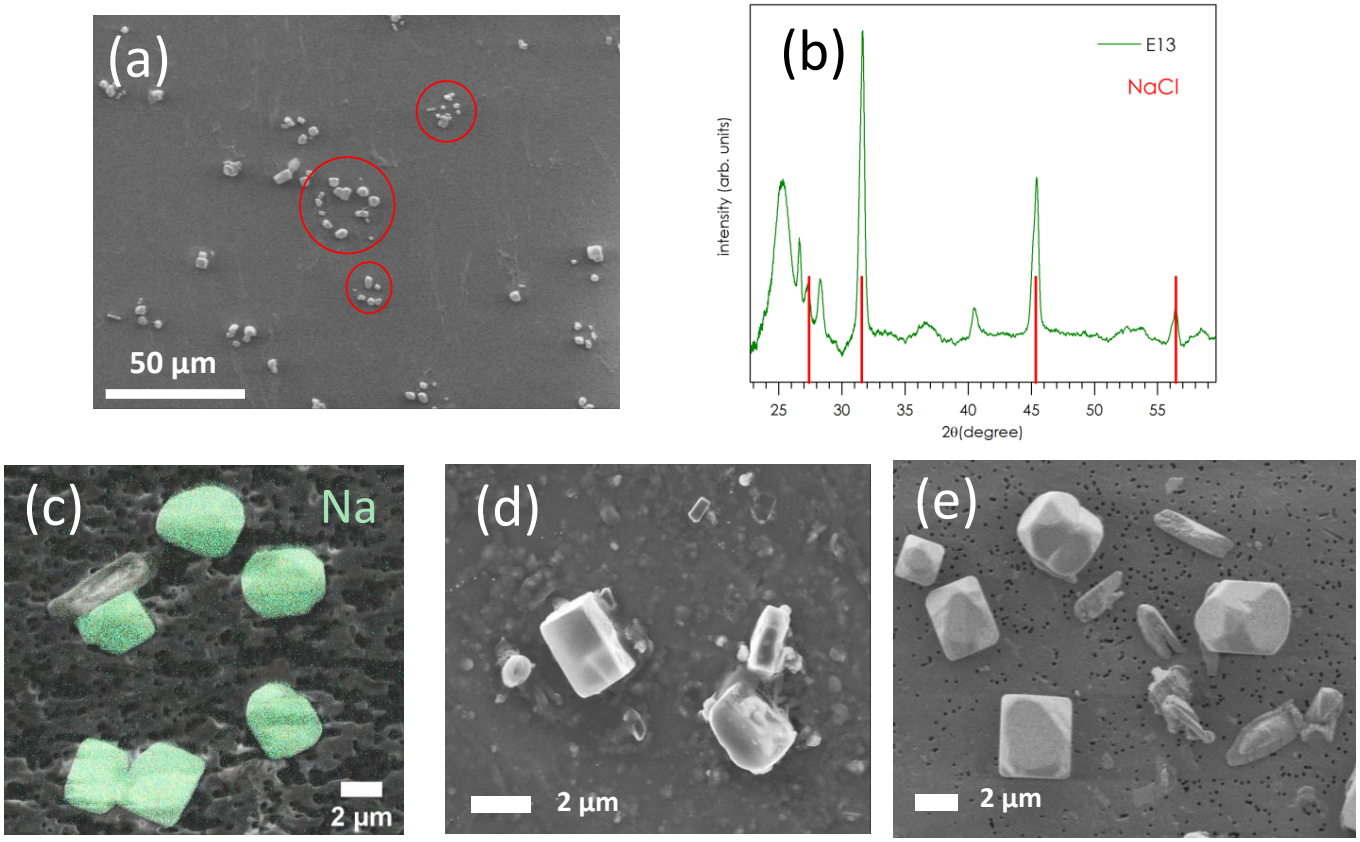

Figure 4. (**a**) SEM image at low magnification of stage E13 (D50% = 9.97 µm) of the P1 sample from Porquerolles (March 2019). (**b**) XRD spectrum of E13-P1; angular positions of NaCl diffraction lines are indicated by red lines. (**c**) SEM image coupled with EDX analysis of sodium of E13-P1. SEM images of (**d**) stage E13 of the P2 sample of Porquerolles (July 2019) and (**e**) stage E13 of the C4 sample from Le Croisic (July 2020), showing similar NaCl crystallites.

3.2. Intermediate Modes

Figure 5a shows a typical SEM image of intermediate modes collected on stages E6–E9 (0.40–1.6 µm). This is stage E7 (D50% = 0.65 µm) of the P1 sample from Porquerolles (March 2019). It is made of a variety of particles of various sizes. NaCl salt crystals are detected (for example, the one surrounded by the green circle), large soot carbon aggregates (white circle), and many other particles of very varied shapes (orange circle). Their EDX analysis (not shown) indicates compositions rich in silicon, aluminum, calcium, oxygen, and sulfur, i.e., they are mineral dusts made of quartz, aluminosilicates (e.g., albite), and gypsum. Figure 5b shows the diffraction diagram of the whole stage E7, where the characteristic lines of both NaCl (halite) and sodium nitrate $NaNO_3$ (nitratine) are observed. In the insert is presented the two-dimensional diffraction image recorded on the detector. The main diffraction peaks of NaCl and $NaNO_3$ appear in the same spatial direction (red circle on the insert), indicating that the two phases coexist in the same crystal, as if they were formed by the growth of one of the phases on the surface of the other, as expected when $NaNO_3$ forms on the surface of dry salt crystals by reaction with atmospheric nitric acid ($NaCl + HNO_3 \rightarrow NaNO_3 + HCl$) [21–23]. For comparison, Figure 5c shows a SEM image of stage E7 of the Porquerolles sampling P2 (July 2019) and Figure 5d shows a SEM image of stage E7 of the Le Croisic sampling C4 (July 2020). In blue are circled metallic particles (steel), in red the sulfate compounds (with calcium and sodium), in white the soot particles, in yellow the carbon particles (microplastics), in orange the mineral particles (mainly calcium carbonate). Similarly to the P1 sample, these two samples exhibit a large variety of particles with both natural origin (mineral particles) and anthropic origin (soot, metallic particles).

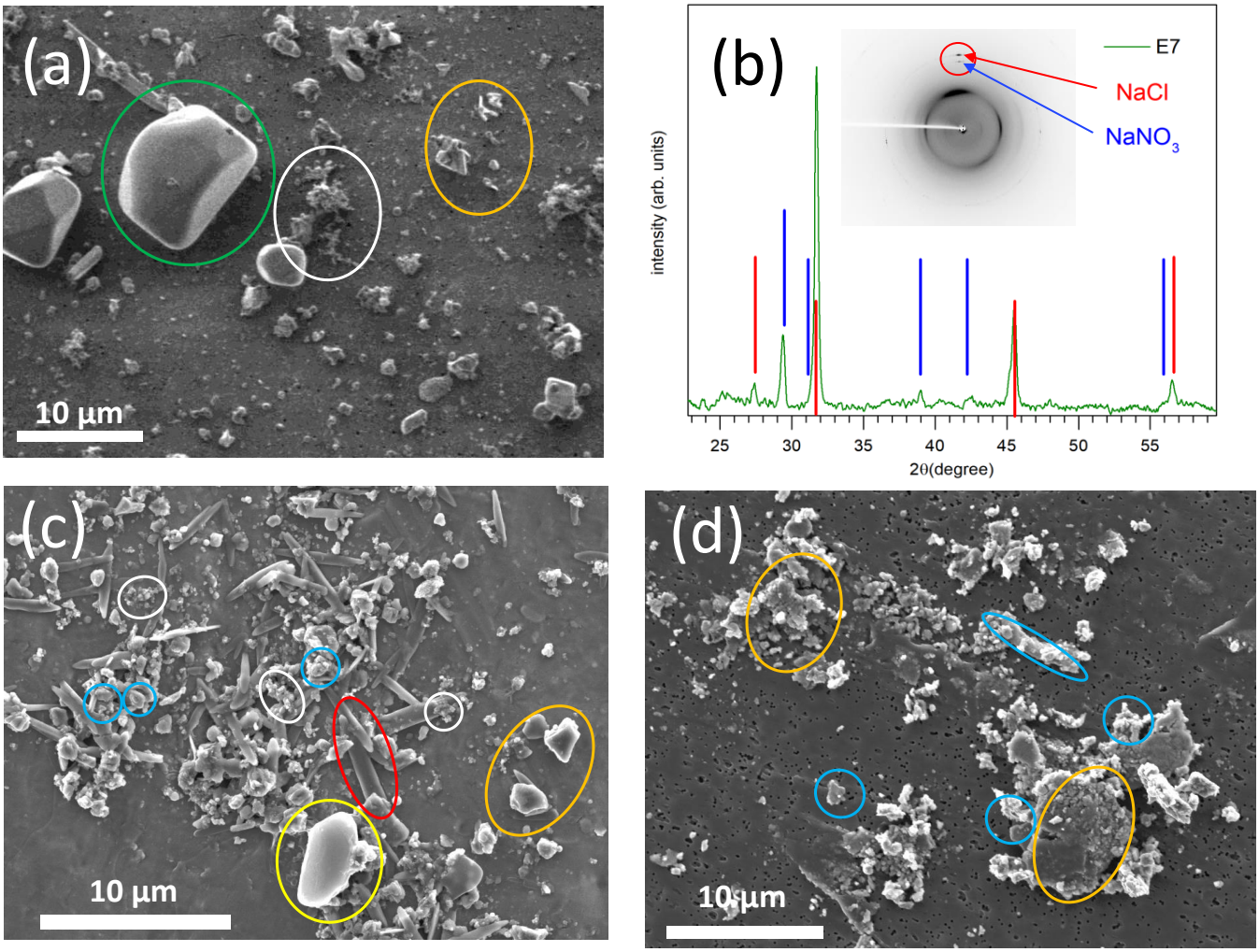

Figure 5. (**a**) SEM image of stage E7 (D50% = 0.65 µm) of Porquerolles sampling P1 (March 2019); the colored circles indicate different types of particles: NaCl salt (green), soot carbon aggregates (white) and mineral particles (alumina, gypsum, etc.) (orange). (**b**) XRD spectrum of stage E7; the angular positions of the NaCl diffraction lines are indicated by red lines, and those of $NaNO_3$ in blue. (**c**) SEM image of stage E7 of Porquerolles sampling P2 (July 2019) and (**d**) stage E7 of Le Croisic sampling C4 (July 2020). On (**c**) and (**d**) are circled in the red sulfate-rich particles, in blue the few metallic particles (steel), in white the soot particles, in yellow the carbon particles (microplastics), and in orange the mineral particles (calcium carbonate).

3.3. Fine Modes

Figure 6 presents selected SEM images of the fine modes stages E1–E5 (D50% = 0.03–0.26 µm) collected on polycarbonate substrates. Figure 6a shows stage E4 (0.17 µm) of the P1 sample at Porquerolles and Figure 6b that of the C4 sample taken at Le Croisic. On both sites, the nature of the particles is the same. They consist of single or fused particles having facets, and soot carbon aggregates. Figure 6c shows the X-ray diffraction pattern collected on the E4 filter of the P1 sample from Porquerolles. The main diffraction peaks correspond to the ammonium sulfate salt $(NH_4)_2SO_4$, whose diffraction positions are indicated by the orange vertical bars that correspond very well to the diffraction file of Mascagnite $(NH_4)_2SO_4$ (JCPDS N° 0-001-0363). Very similar SEM observations of sulfate aerosol particles from sea-spray have been reported [24]. Statistical measurements of SEM images of the E4 stage of P1 and C4 samplings indicate an average median diameter of the sulfate particles of 0.56 ± 0.20 µm for P1 and 0.26 ± 0.12 µm for C4. This is typical of submicronic non-sea-salt sulfate aerosol formed from combustion or biogenic source,

while sulfate particles of marine origin (from sea-spray and biogenic dimethyl sulfide) are supermicronic [25]. The SEM image of the region of the E4 stage of C4 presented in Figure 6b has been chosen for the presence of large particles, allowing easier EDX maps of the N, O, and S elements, which are presented in Figure 6d; however, the size of those large particles is not representative of the average particle size of 0.26 ± 0.12 µm. These maps confirm that these particles are made of ammonium sulfate salts $(NH_4)_2SO_4$ and are at the origin of the X-ray diffraction diagram presented in Figure 6c. These particles are typical of reactions between nss-SO_4^{2-} aerosols of marine origin and ammonium NH_4^+ coming from polluted continental air masses [26]:

$$H_2SO_4 + NH_3 \rightarrow NH_4HSO_4 \quad (1)$$

$$NH_4HSO_4 + NH_3 \rightarrow (NH_4)_2SO_4 \quad (2)$$

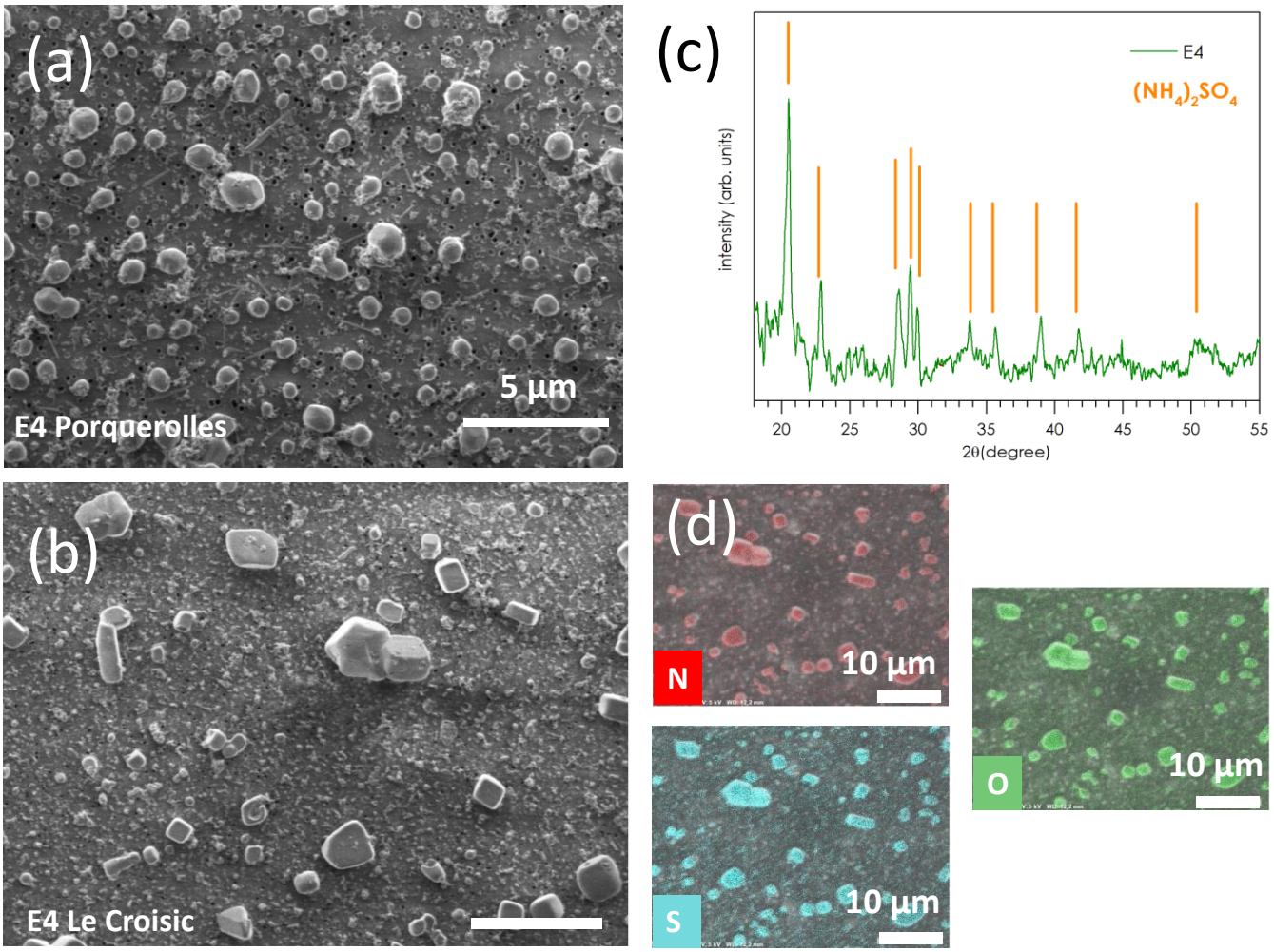

Figure 6. (a) SEM image of the E4 stage (D50% = 0.17 µm) of the Porquerolles sample P1 and (**b**) of the Le Croisic sample C4. (**c**) XRD spectrum of the E4 stage of the P1 sample; the angular positions of the diffraction lines of $(NH_4)_2SO_4$ are indicated by orange lines. (**d**) EDX maps of the N, O, and S elements of the E4 filter of the C4 sample presented in (**b**).

Figure 7 shows further high magnification SEM images of the E4 stages of the C4 sample from Le Croisic (Figure 7a) and Porquerolles (Figure 7b), where soot aggregates coexisting with sulfate salt particles can be better distinguished. The Raman spectrum of the E4 stage of Le Croisic (Figure 7c, red) presents an intense contribution of soot (at 1315, 1445 and 1604 cm^{-1}) [27] along with fine bands in the region 400–1200 cm^{-1} (insert of

Figure 7c) associated with ammonium sulfate salts $(NH_4)_2SO_4$ (451, 622, 975 cm^{-1}), sodium sulfate Na_2SO_4 (644, 1131 cm^{-1}), and sodium nitrate $NaNO_3$ (1066 cm^{-1}). These salts' aerosols usually form the most numerous classes of submicronic particles in the marine boundary layer [25,27–31], while potassium sulfate K_2SO_4 (449, 454, 983 cm^{-1}) is a tracer of smoke from biomass burning.

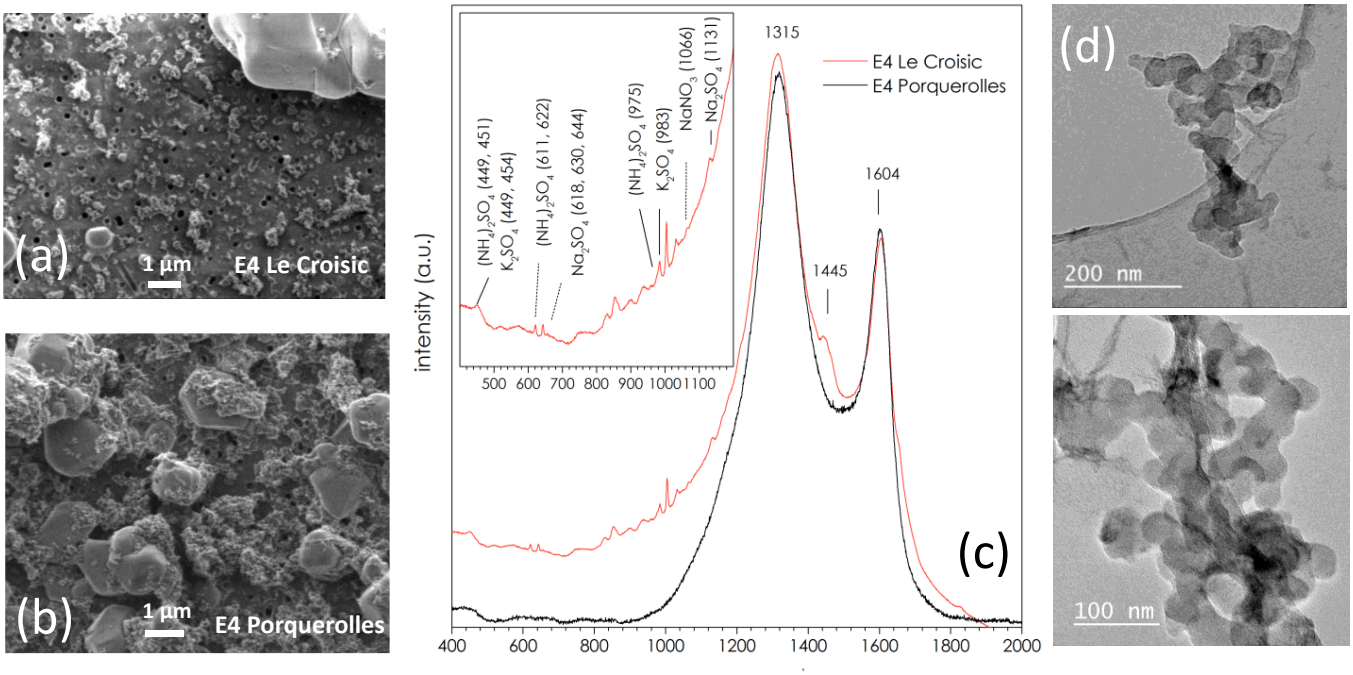

Figure 7. (**a**) High magnification SEM image of the E4 stage (D50% = 0.17 µm) of the C4 sample from Le Croisic and (**b**) the P1 sample from Porquerolles. (**c**) Raman spectra of the same samples, carried out on the aluminum part of the E4 stages. (**d**) TEM image of soot aggregates extracted from the E4 filter of P1.

The Raman spectrum of the E4 stage of Porquerolles (Figure 7c, black) is dominated by the contribution of soot. Contributions from the salts are probably too weak to be detected, since they are clearly observed in SEM. Figure 7d shows a TEM image of soot aggregates extracted from the E4 filter, whose fractal morphology is typical of carbon soot [27].

Figure 8 presents several samples of the E3 stage taken at Le Croisic in different air-mass conditions. Figure 8a shows optical photographs of the E3 polycarbonate filters issued from three samples acquired during an oceanic (C4), coastal (C7), and continental (C5) wind direction, respectively, and similar wind speed. The black dots arranged in semicircles—clearly visible on the C7 and C5 samples—are the impaction points, located beneath the metal sieve of stage E4 of the impactor. The soot particles are at the origin of the black color of these points of impact. They are much denser on the C5 sample (continental) than on the C4 sample (oceanic). A measurement of the particle density per unit area was carried out by analysis of several SEM images of each sample (Figure 8b). We see that the continental air mass (C5) is about four times more loaded with fine particles than the oceanic air mass, and that the densities of particles collected from the coastal air masses are intermediate. This is probably due the fact that the coastal sample densities, i.e., C6 and C7, result from a mixture of the two influences. We can therefore conclude that the origin of the air mass influences the density of particles collected, but has no effect on their nature, which remains, in this case, made of sulfate salts and carbon soot.

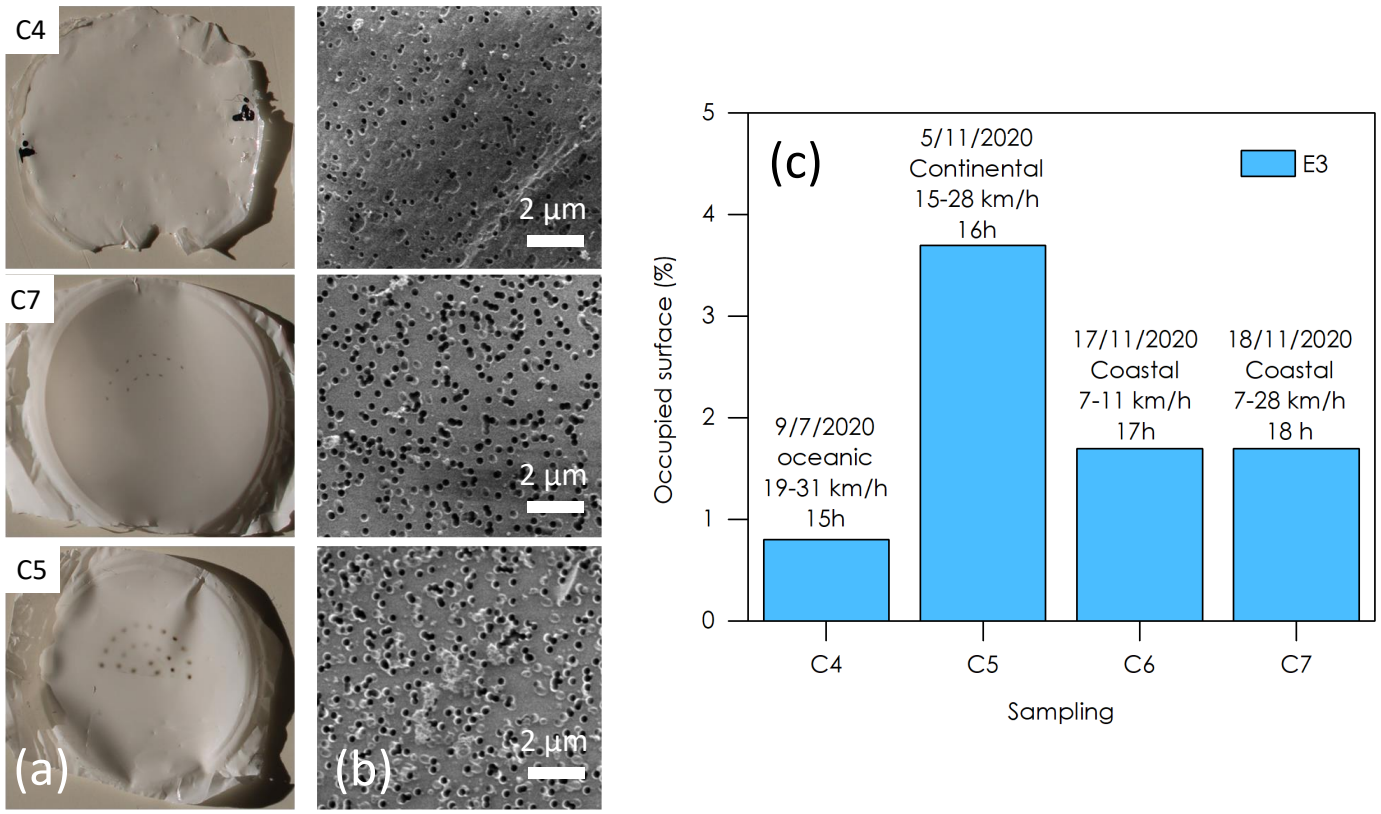

Figure 8. (**a**) Photograph of the polycarbonate filters of the E3 stages of three samples taken at Le Croisic under different air mass conditions: oceanic (C4), continental (C5), and costal (C7). (**b**) Typical SEM images used for particle density measurements. (**c**) Particle density per unit area for 4 samples from Le Croisic (C4, C5, C6, and C7).

We have already illustrated the consistency of the physico-chemical nature of the samples over time by the SEM images shown in Figures 4 and 5 for the coarse (E13) and intermediate (E7) modes of samples P1, P2, and C4, and Figure 6 for the fine (E4) modes of samples P1 and C4. As additional evidence of this consistency, Figure 9 shows the coarse (E13), intermediate (E7), and fine (E4) mode stages of samples C6 and C7 sampled at Le Croisic. Similar to the other samplings, the coarse mode (Figure 9a,d) is made of NaCl crystals (green circles), the intermediate mode (Figure 9b,e) is made of a mixture of salts, large soot aggregates (white circles), and minerals (orange circles), and the fine mode (Figure 9c,f) is made of soot and sulfate particles (red circles).

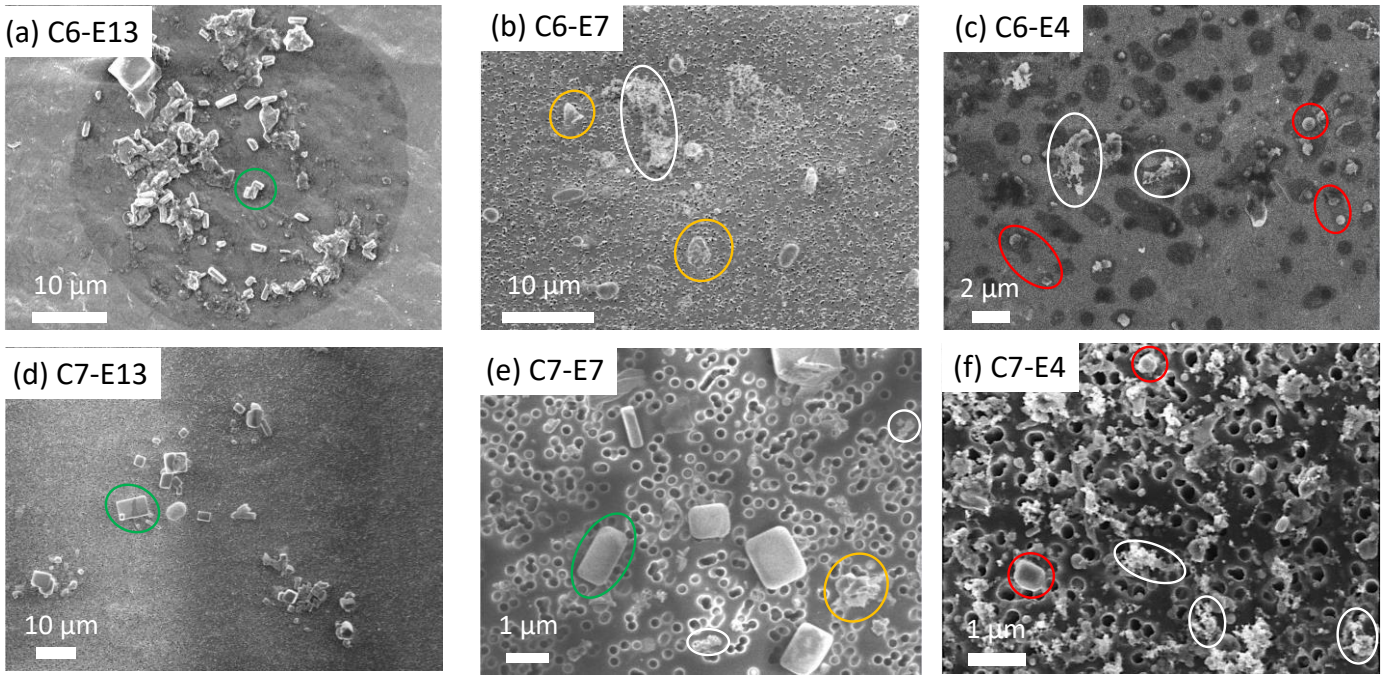

Figure 9. SEM images of the coarse (E13), intermediate (E7) and fine (E4) modes stages of samples C6 (**a**–**c**), and C7 (**d**–**f**) of Le Croisic. The coarse modes (**a**,**d**) are made of NaCl salt crystals (green circles), the intermediate modes (**b**,**e**) of a mixture of salts, large soot aggregates (white circles), and minerals (orange circles), and the fine modes (**c**,**f**) of soot and sulfate particles (red circles).

4. Discussion and Conclusions

The present results deal with aerosol analysis based on the non-intrusive and nondestructive methodology. The aerosol samplings can be thus further analyzed in the future with other analytical tools, giving a sustainable development character to our methodology. In addition, while aerosol concentrations and compositions were investigated in many Mediterranean areas in several studies using chemical analytical techniques (ion chromatography, thermo-optical analysis, X-ray fluorescence, etc.), no direct observation of the particulate matter was carried out. The present study makes it possible to physically materialize those aerosol particles then named "nss-SO4", "black carbon", "dust", etc., following their chemical compositions, but not directly observed as physical particles.

Despite the different meteorological characteristics of the two study areas, our results show that the collected samples in the two sites are very similar. The present analysis is based on samples analyzed at two locations and at different times. This random sampling provided the same qualitative composition six times in a row (P1, P2, C4–C7), indicating a good reproducibility. We can trust that the analysis of the aerosol composition would not be different using more samples, more particularly concerning the coarse portion of the aerosol spectrum, which is constituted by sea-salt and the finer one (i.e., essentially soot and sulfates). On the intermediate sizes, however, it should be noted that small differences occur from one sample to another. The nature of these particles does not vary significantly with the season for Porquerolles and Le Croisic, or the origin of the air mass for Le Croisic. On the other hand, the samples from Le Croisic, of oceanic character, showed that the number of these particles vary according to the origin of the air masses, the air of continental origin being more loaded with fine particles than the air of oceanic origin. In both areas, we observed a persistent background of soot particles and sulfate salt particles. This shows the important contribution of the non-sea-salt sulfates and anthropogenic particles issued from petrogenic emissions related to transportation (ships, cars, trucks), urban heating, etc. Intermediate sizes (0.2 µm < d < 1 µm) are constituted of salt crystals aged by interaction with nitric acid, some large soot aggregates, and mineral particles (silica, gypsum, etc.),

from soil erosion, etc., while NaCl crystals are left by drying drops of sea salt aerosols. Finally, our results also show that no internal mixing occurs between solid particles of the coarse modes (>1 μm).

The present results indicate a rather homogeneous marine background concentration over the Mediterranean Sea by comparison with aerosol concentrations found in the Eastern Mediterranean [8,9] and shows the occurrence of the external mixing between sea-spray, which represents quite large aerosols, and anthropogenic matter during the atmospheric transport. In addition, under the anthropogenic influence, corresponding more particularly to air masses of continental origin, our methodology confirms the level of atmospheric carbonaceous concentrations noted in such coastal sites of the central Mediterranean [32]. Assuming that the organic carbon is mainly part of carbon soot, our results confirm the higher contribution of organics in the French Mediterranean coast compared to the ones observed in the Eastern Mediterranean for the summer and winter seasons [8] and in the Northern Adriatic [11].

Author Contributions: Conceptualisation, P.P. and C.L.; Methodology: D.F. and O.G.; Formal analysis: P.P., V.T., C.L. and J.P.; Writing: P.P. and J.P.; Original draft: P.P. and J.P.; Software: A.L. and T.M. All authors have read and agreed to the published version of the manuscript.

Funding: This work was sponsored by ANR-ASTRID under contract ANR-18-ASTR-0002.

Institutional Review Board Statement: Not applicable.

Informed Consent Statement: Not applicable.

Data Availability Statement: Not applicable.

Acknowledgments: This work was sponsored by ANR-ASTRID under contract ANR-18-ASTR-0002. The authors wish to thank Antoine Bertholon, Arnaud Blangy, and Yves Perignon of the SEM-RV for their help to the experimental effort in Le Croisic.

Conflicts of Interest: The authors declare no conflict of interest.

References

1. Textor, C.; Schulz, M.; Guibert, S.; Kinne, S.; Balkanski, Y.; Bauer, S.; Berntsen, T.; Berglen, T.; Boucher, O.; Chin, M.; et al. Analysis and quantification of the diversities of aerosol life cycles within AeroCom. *Atmos. Chem. Phys.* **2006**, *6*, 1777–1813. [CrossRef]
2. Schwartz, J.; Dockery, D.W. Particulate Air Pollution and Daily Mortality in Steubenville, Ohio. *Am. J. Epidemiol.* **1992**, *135*, 12–19. [CrossRef]
3. Dockery, D.W.; Pope, C.A. Acute Respiratory Effects of Particulate Air Pollution. *Annu. Rev. Public Health* **1994**, *15*, 107–132. [CrossRef] [PubMed]
4. European Environment Agency. *Air Quality in Europe*; EEA Report No 10/2019; Publications Office of the European Union: Luxembourg, 2019. Available online: https://www.eea.europa.eu/publications/air-quality-in-europe-2019 (accessed on 27 November 2022).
5. Giorgi, F.; Lionello, P. Climate change projections for the Mediterranean region. *Glob. Planet. Chang.* **2008**, *63*, 90–104. [CrossRef]
6. Piazzola, J.; Sellegri, K.; Bourcier, L.; Mallet, M.; Tedeschi, G.; Missamou, T. Physicochemical characteristics of aerosols measured in the spring time in the Mediterranean coastal zone. *Atmos. Environ.* **2012**, *54*, 545–556. [CrossRef]
7. Knipping, E.M.; Dabdub, D. Impact of Chlorine Emissions from Sea-Salt Aerosol on Coastal Urban Ozone. *Environ. Sci. Technol.* **2003**, *37*, 275–284. [CrossRef]
8. Bardouki, H.; Liakakou, H.; Economou, C.; Sciare, J.; Smolík, J.; Ždímal, V.; Eleftheriadis, K.; Lazaridis, M.; Dye, C.; Mihalopoulos, N. Chemical composition of size-resolved atmospheric aerosols in the eastern Mediterranean during summer and winter. *Atmos. Environ.* **2003**, *37*, 195–208. [CrossRef]
9. Eleftheriadis, K.; Colbeck, I.; Housiadas, C.; Lazaridis, M.; Mihalopoulos, N.; Mitsakou, C.; Smolík, J.; Ždímal, V. Size distribution, composition and origin of the submicron aerosol in the marine boundary layer during the eastern Mediterranean "SUB-AERO" experiment. *Atmos. Environ.* **2006**, *40*, 6245–6260. [CrossRef]
10. Schembari, C.; Bove, M.C.; Cuccia, E.; Cavalli, F.; Hjorth, J.; Massabò, D.; Nava, S.; Udisti, R.; Prati, P. Source apportionment of PM10 in the Western Mediterranean based on observations from a cruise ship. *Atmos. Environ.* **2014**, *98*, 510–518. [CrossRef]
11. Piazzola, J.; Mihalopoulos, N.; Canepa, E.; Tedeschi, G.; Prati, P.; Zarmpas, P.; Bastianini, M.; Missamou, T.; Cavaleri, L. Characterization of aerosols above the Northern Adriatic Sea: Case studies of offshore and onshore wind conditions. *Atmos. Environ.* **2016**, *132*, 153–162. [CrossRef]

12. Ovadnevaite, J.; Manders, A.; de Leeuw, G.; Ceburnis, D.; Monahan, C.; Partanen, A.-I.; Korhonen, H.; O'Dowd, C.D. A sea spray aerosol flux parameterization encapsulating wave state. *Atmos. Meas. Technol.* **2014**, *14*, 1837–1852. [CrossRef]
13. Lewis, E.R.; Schwartz, S.E. *Sea Salt Aerosol Production: Mechanisms, Methods, Measurements and Models-A Critical Review*; Geophysical Monogr. Ser. 152; AGU: Washington, DC, USA, 2004; p. 413.
14. Andreas, E.L. A new sea spray generation function for wind speeds up to 32 m/s. *J. Phys. Oceanogr.* **1998**, *28*, 2175–2184. [CrossRef]
15. Zieger, P.; Väisänen, O.; Corbin, J.C.; Partridge, D.G.; Bastelberger, S.; Mousavi-Fard, M.; Rosati, B.; Gysel, M.; Krieger, U.K.; Leck, C.; et al. Revising the hygroscopicity of inorganic sea salt particles. *Nat. Commun.* **2017**, *8*, 15883. [CrossRef] [PubMed]
16. Swietlicki, E.; Hansson, H.-C.; Hämeri, K.; Svenningsson, B.; Massling, A.; McFiggans, G.; McMurry, P.H.; Petäjä, T.; Tunved, P.; Gysel, M.; et al. Hygroscopic properties of submicrometer atmospheric aerosol particles measured with H-TDMA instruments in various environments—A review. *Tellus B Chem. Phys. Meteorol.* **2008**, *60*, 432. [CrossRef]
17. Wang, X.; Sultana, C.M.; Trueblood, J.; Hill, T.C.J.; Malfatti, F.; Lee, C.; Laskina, O.; Moore, K.A.; Beall, C.M.; McCluskey, C.S.; et al. Microbial control of sea spray aerosol composition: A tale of two blooms. *ACS Cent. Sci.* **2015**, *1*, 124–131. [CrossRef]
18. Piazzola, J.; Despiau, S. Contribution of marine aerosols in the particle size distributions observed in Mediterranean coastal zone. *Atmos. Environ.* **1997**, *31*, 2991–3009. [CrossRef]
19. Rolph, G.; Stein, A.; Stunder, B. Real-time Environmental Applications and Display sYstem: READY. *Environ. Model. Softw.* **2017**, *95*, 210–228. [CrossRef]
20. Efstratiou, M.; Christy, J.; Khellil, S. Crystallization-Driven Flows within Evaporating Aqueous Saline, Droplets. *Langmuir* **2020**, *36*, 4995–5002. [CrossRef]
21. Gard, E.E.; Kleeman, M.J.; Gross, D.S.; Hughes, L.S.; Allen, J.O.; Morrical, B.D.; Fergenson, D.P.; Dienes, T.; Gälli, M.E.; Johnson, R.J.; et al. Direct observation of heterogeneous chemistry in the atmosphere. *Science* **1998**, *279*, 1184–1187. [CrossRef]
22. Laskin, A.; Gaspar, D.J.; Wang, W.; Hunt, S.W.; Cowin, J.P.; Colson, S.D.; Finlayson-Pitts, B.J. Reactions at Interfaces As a Source of Sulfate Formation in Sea-Salt Particles. *Science* **2003**, *301*, 340–344. [CrossRef]
23. Ault, A.P.; Guasco, T.L.; Baltrusaitis, J.; Ryder, O.S.; Trueblood, J.V.; Collins, D.B.; Ruppel, M.J.; Cuadra-Rodriguez, L.A.; Prather, K.A.; Grassian, V.H. Heterogeneous reactivity of nitric acid with nascent sea spray aerosol: Large differences observed between and within individual particles. *J. Phys. Chem. Lett.* **2014**, *5*, 2493–2500. [CrossRef]
24. Ganor, E.; Levin, Z.; Van Grieken, R. Composition of individual aerosol particles above the Israelian Mediterranean coast during the summertime. *Atmos. Environ.* **1998**, *32*, 1631–1642. [CrossRef]
25. Milford, J.B.; Davison, C.I. The sizes of particulate sulfate and Nitrate in the atmosphere—A review. *JAPCA* **1987**, *37*, 125–134. [CrossRef]
26. Sellegri, K.; Gourdeau, J.; Putaud, J.P.; Despiau, S. Chemical composition of marine aerosol in a Mediterranean coastal zone during the FETCH experiment. *J. Geophys. Res.* **2001**, *106*, 12036–12037. Available online: https://agupubs.onlinelibrary.wiley.com/doi/pdf/10.1029/2000JD900629 (accessed on 27 November 2022).
27. Parent, P.; Laffon, C.; Marhaba, I.; Ferry, D.; Regier, T.Z.; Ortega, I.K.; Chazallon, B.; Carpentier, Y.; Focsa, C. Nanoscale characterization of aircraft soot: A high-resolution transmission electron microscopy, Raman spectroscopy, X-ray photoelectron and near-edge X-ray absorption spectroscopy study. *Carbon* **2016**, *101*, 86–100. [CrossRef]
28. Matsumura, T.; Hayashi, M. Hygroscopic growth of an $(NH_4)_2SO_4$ aqueous solution droplet measured using an Environmental Scanning Electron Microscope (ESEM). *Aerosol Sci. Technol.* **2007**, *41*, 770–774. [CrossRef]
29. Johnson, S.A.; Kumar, R. Composition and spectral characteristics of ambient aerosol at Mauna Loa Observatory. *J. Geophys. Res.* **1991**, *96*, 5379–5386. [CrossRef]
30. Murphy, D.M.; Anderson, J.R.; Quilnn, P.K.; Mclnnes, L.M.; Brechtel, F.J.; Kreidenwels, S.M.; Middlebrook, A.M.; Pósfai, M.; Thomson, D.S.; Buseck, P.R. Influence of sea-salt on aerosol radiative properties in the Southern Ocean marine boundary layer. *Nature* **1998**, *392*, 62–65. [CrossRef]
31. Hoppel, W.A.; Frick, G.M.; Fitzgerald, J.W. Deducing droplet concentration and supersaturation in marine boundary layer clouds from surface aerosol measurements. *J. Geophys. Res. Atmos.* **1996**, *101*, 26553–26565. [CrossRef]
32. Perrone, M.R.; Piazzalunga, A.; Prato, M.; Carofalo, I. Composition of fine and coarse particles in a coastal site of the central Mediterranean: Carbonaceous species contributions. *Atmos. Environ.* **2011**, *45*, 7470–7477. [CrossRef]